THE JOURNAL OF BIOLOGICAL CHEMISTRY VOL. 290, NO. 46, pp. 27460–27472, November 13, 2015
© 2015 by The American Society for Biochemistry and Molecular Biology, Inc. Published in the U.S.A.

Perturbation of the Vacuolar ATPase

*A NOVEL CONSEQUENCE OF INOSITOL DEPLETION**

Received for publication, August 5, 2015 Published, JBC Papers in Press, August 31, 2015, DOI 10.1074/jbc.M115.683706

Rania M. Deranieh[‡], Yihui Shi[‡], Maureen Tarsio[§], Yan Chen[‡], J. Michael McCaffery[¶], Patricia M. Kane[§], and Miriam L. Greenberg[‡1]

From the [‡]Department of Biological Sciences, Wayne State University, Detroit, Michigan 48202, the [§]Department of Biochemistry and Molecular Biology, State University of New York Upstate Medical University, Syracuse, New York 13210, and the [¶]Integrated Imaging Center, Department of Biology, Johns Hopkins University, Baltimore, Maryland 21218

Background: Inositol is essential for viability, but its role in vacuolar function has not been previously characterized.
Results: Inositol depletion and valproate compromise $PI3,5P_2$ homeostasis and perturb vacuolar function.
Conclusion: Both inositol depletion and valproate perturb the V-ATPase.
Significance: Understanding the cellular consequences of inositol depletion may provide insight into the therapeutic mechanism of action of the anticonvulsant drug valproate.

Depletion of inositol has profound effects on cell function and has been implicated in the therapeutic effects of drugs used to treat epilepsy and bipolar disorder. We have previously shown that the anticonvulsant drug valproate (VPA) depletes inositol by inhibiting *myo*-inositol-3-phosphate synthase, the enzyme that catalyzes the first and rate-limiting step of inositol biosynthesis. To elucidate the cellular consequences of inositol depletion, we screened the yeast deletion collection for VPA-sensitive mutants and identified mutants in vacuolar sorting and the vacuolar ATPase (V-ATPase). Inositol depletion caused by starvation of *ino1*Δ cells perturbed the vacuolar structure and decreased V-ATPase activity and proton pumping in isolated vacuolar vesicles. VPA compromised the dynamics of phosphatidylinositol 3,5-bisphosphate ($PI3,5P_2$) and greatly reduced V-ATPase proton transport in inositol-deprived wild-type cells. Osmotic stress, known to increase $PI3,5P_2$ levels, did not restore $PI3,5P_2$ homeostasis nor did it induce vacuolar fragmentation in VPA-treated cells, suggesting that perturbation of the V-ATPase is a consequence of altered $PI3,5P_2$ homeostasis under inositol-limiting conditions. This study is the first to demonstrate that inositol depletion caused by starvation of an inositol synthesis mutant or by the inositol-depleting drug VPA leads to perturbation of the V-ATPase.

Inositol is a ubiquitous cyclitol that is required for the synthesis of numerous biologically important compounds. Cells derive inositol from three sources as follows: import from the extracellular medium; recycling of inositol 1,4-bisphosphate, which is derived from inositol 1,4,5-triphosphate, a by-product of the breakdown of phosphatidylinositol 4,5-bisphosphate; and from *de novo* biosynthesis from glucose 6-phosphate (Glc-6-P).[2] In yeast, inositol supplementation triggers a global transcriptional response, where hundreds of genes have been shown to be regulated by inositol, including phospholipid biosynthesis genes that harbor the upstream activating sequence (UAS_{INO}) in their promoters (1–4). Inositol compounds, including inositol phosphates, phosphoinositides, ceramides, and glycosylphosphatidylinositol (GPI), have many structural and functional roles that include membrane biogenesis, membrane trafficking, signal transduction, gene expression, and cytoskeletal organization. Therefore, depletion of inositol has profound effects on cells (5). In addition to causing alteration of lipid biosynthesis (6) and a decrease in phosphoinositides (7–9), depletion of inositol results in activation of stress response pathways, including the PKC and the unfolded protein response pathways (10–12).

Inositol depletion has been implicated in the therapeutic mechanisms of drugs used to treat bipolar disorder. The inositol depletion hypothesis proposed by Berridge (13) posits that depletion of inositol caused by lithium leads to a decrease in inositol 1,4,5-triphosphate-mediated signaling and dampening of the PI cycle. We have previously shown that valproate (VPA), a branched, short-chain fatty acid used for the treatment of epilepsy (14), bipolar disorder (15), and migraine (16), depletes inositol in yeast (17) by increasing the phosphorylation of *myo*-inositol-3-phosphate synthase, the enzyme that catalyzes the first and rate-limiting step in inositol biosynthesis (18). The mechanism that underlies the therapeutic efficacy of VPA is not known. Thus, elucidating the cellular consequences of inositol depletion could identify the mechanism of action whereby VPA elicits its therapeutic effect. Perturbation of inositol and phosphoinositide metabolism is associated with several disorders, including bipolar disorder (19), Alzheimer disease (20, 21), Lowe syndrome (22), X-linked myotubular myopathy (23), and

* This work was supported, in whole or in part, by National Institutes of Health Grant DK 081367 (to M. L. G.) and Grant GM 50322 (to P. M. K.). This work was also supported by a Fulbright Scholarship, a Wayne State University Graduate Research Fellowship, and Graduate Research Funds (to R. M. D.). The authors declare that they have no conflicts of interest with the contents of this article.

[1] To whom correspondence should be addressed: Dept. of Biological Sciences, Wayne State University, 5047 Gullen Mall, Detroit, MI 48202. Tel.: 313-577-5202; Fax: 313-577-6891; E-mail: mlgreen@sun.science.wayne.edu.

[2] The abbreviations used are: Glc-6-P, glucose 6-phosphate; V-ATPase, vacuolar ATPase; VPA, valproate; PI3P, phosphatidylinositol 3-phosphate, $PI3,5P_2$, phosphatidylinositol 3,5-bisphosphate; SM, synthetic medium; BCECF-AM, 2′,7′-bis(carboxyethyl)-5,6-carboxyfluorescein acetoxymethyl ester.

TABLE 1
Strains used in this study

Strains	Genotype	Source/Ref.
BY4741	*MATa, his 3Δ1, leu 2Δ0, met 15Δ0, ura 3Δ0*	Invitrogen
*ino1*Δ	*MATa, his 3Δ1, leu 2Δ0, met 15Δ0, ura 3Δ0, ino1*Δ*::KanMX4*	Invitrogen
*vma3*Δ	*MATa, his 3Δ1, leu 2Δ0, met 15Δ0, ura 3Δ0, vma3*Δ*::KanMX4*	Invitrogen
*vma9*Δ	*MATa, his 3Δ1, leu 2Δ0, met 15Δ0, ura 3Δ0, vma9*Δ*::KanMX4*	Invitrogen
*vma11*Δ	*MATa, his 3Δ1, leu 2Δ0, met 15Δ0, ura 3Δ0, vma11*Δ*::KanMX4*	Invitrogen
*vma16*Δ	*MATa, his 3Δ1, leu 2Δ0, met 15Δ0, ura 3Δ0, vma16*Δ*::KanMX4*	Invitrogen
*vph1*Δ	*MATa, his 3Δ1, leu 2Δ0, met 15Δ0, ura 3Δ0, vph1*Δ*::KanMX4*	Invitrogen
*stv1*Δ	*MATa, his 3Δ1, leu 2Δ0, met 15Δ0, ura 3Δ0, stv1*Δ*::KanMX4*	Invitrogen
*fab1*Δ	*MATα, his 3Δ1, leu 2Δ0, lys 2Δ0, ura 3Δ0, fab1*Δ*::KanMX4*	Invitrogen
FGY3	*MATα, ura3-52, lys2-801,ade2-101, trp1*Δ*1, his3*Δ*200, leu2*Δ*1*	86
LN284	*MATa leu2–3,112 trp1-1 ura3-52 his4 can1*^{r} *ino1::KanMX*	87

type 2 diabetes (24, 25). Dysfunction of the phosphoinositide $PI3,5P_2$ is specifically associated with the genetic disorders Charcot-Marie-Tooth disease (26) and fleck corneal dystrophy (27).

$PI3,5P_2$ is the signature phosphoinositide of the vacuole (the yeast lysosome) (28). It is generated from phosphatidylinositol 3-phosphate (PI3P) by the sole conserved kinase Fab1p (the homolog of PIKfyve), which is positively regulated by Vac7p and Vac14p (29–31). Fab1p, along with its known regulators, forms part of a protein complex that localizes to the vacuolar membrane during $PI3,5P_2$ synthesis (32, 33). The regulated synthesis and turnover of $PI3,5P_2$ is proposed to underlie many aspects of vacuole function (34), including regulation of vacuolar ion transport, membrane efflux, membrane turnover, and signaling (34–37). Although $PI3,5P_2$ makes up less than 0.1% of all phosphoinositides (38), its absence from the cell has a profound effect on cell structure and function. The *fab1*Δ mutant (which cannot synthesize $PI3,5P_2$) exhibits enlarged vacuoles, reduced vacuolar acidification, and perturbed trafficking. The mechanism that leads to these phenotypes is not fully understood. However, loss of $PI3,5P_2$ compromises V-ATPase activity and assembly (34). In the same context, Baars *et al.* (35) showed that acidification of the vacuole is crucial for vacuolar fission, suggesting that $PI3,5P_2$ supports vacuolar fission by regulating V-ATPase activity.

The V-ATPase is an ATP-driven proton pump that plays a significant role in maintaining pH homeostasis necessary for the function of vacuoles and other organelles (39). It mediates proton transport across membranes to acidify intracellular organelles and regulates the ionic balance within cells (40). Present in the plasma membranes of specialized cells, the V-ATPase also helps regulate extracellular pH (41). In osteoclasts, the V-ATPase facilitates bone resorption (42, 43). In kidney cells, it is involved in the regulation of systemic acid-base balance (44). Neuronal cells require the V-ATPase for uptake and storage of neurotransmitters in synaptic vesicles (45, 46). The V-ATPase is also required in neurons for endocytosis (47), exocytosis (48), and neurotransmitter release (49, 50). The mechanism that links $PI3,5P_2$ to V-ATPase is not fully understood, but a recent study by Li *et al.* (51) showed that $PI3,5P_2$ may bind to the V_0 sector and activate the V-ATPase by stabilizing V_1-V_0 interactions.

In this study, we examined the cellular consequences of inositol depletion caused by VPA. We show that inositol depletion, induced genetically (by starving inositol auxotrophs) or by VPA treatment, disrupts $PI3,5P_2$ homeostasis and causes a decrease in V-ATPase activity and H^+ pumping. This is the first report to implicate inositol levels in the regulation of the V-ATPase and suggests a possible new therapeutic target of VPA.

Experimental Procedures

Strains, Media, and Growth Conditions—The *Saccharomyces cerevisiae* strains used in this work are listed in Table 1. Cells were maintained on YPD medium (1% yeast extract, 2% bactopeptone, and 2% glucose). For growth of the deletion mutants, the medium was supplemented with G418 (200 μg/ml). Synthetic minimal medium (SM) contained all the essential components of Difco® yeast nitrogen base (minus inositol), 2% glucose, 0.2% ammonium sulfate, vitamins, the four amino acids histidine (20 mg/liter), leucine (60 mg/liter), methionine (20 mg/liter), and lysine (20 mg/liter), and the nucleobase uracil (40 mg/liter). Where indicated, inositol was used at a concentration of 75 μM (I+). For selection of cells carrying plasmids, appropriate amino acids were omitted. For solid media, 2% agar was added. To starve cells for inositol, *ino1*Δ cells were grown overnight in SM supplemented with inositol, harvested, washed twice in distilled H_2O, and resuspended in inositol-free medium (I−). For osmotic stress experiments, media were supplemented with 0.9 M NaCl. Growth in liquid cultures was monitored spectrophotometrically by measuring absorbance at 550 nm. All incubations were at 30 °C unless otherwise stated.

Screening for Sensitivity to VPA—The BY4741 *MATa* haploid yeast deletion collection containing deletions of non-essential genes (4,815 strains) was used for this screen. Cells were precultured in 96-well microtiter plates in YPD supplemented with 15% glycerol and G418 (200 μg/ml). A sterilized 96-pin replicator was used to inoculate 96-microwell plates containing synthetic complete medium supplemented with 2, 3, and 6 mM VPA. For the control, no VPA was added. Plates were incubated at 30 °C for 5 days. Growth was scored relative to that of wild-type BY4741. Cultures that showed less growth than wild-type in the presence of 2–3 mM VPA were considered to be hypersensitive. To examine whether sensitivity was due to inositol depletion, drug sensitivity was tested in the presence or absence of inositol.

Cytosolic and Vacuolar pH Measurement—Cytosolic pH was measured using the yeast pHluorin, a pH-sensitive and ratiometric green fluorescent protein (52). Wild-type cells were transformed with the construct pPGK-pHluorin, in which the yeast pHluorin is under control of a phosphoglycerate kinase promoter, a generous gift from Dr. Rajini Rao (Johns Hopkins University). Transformants were selected on SM lacking uracil

and checked for fluorescence before every experiment. Cells were grown to the mid-log phase in selective SM in I+ or I−, in the presence of different concentrations of VPA. Cells were harvested by centrifugation, washed, and resuspended in 50 mM MES buffer (50 mM MES, 50 mM HEPES, 50 mM KCl, 50 mM NaCl, 0.2 M NH_4 acetate, 10 mM NaN_3, 10 mM 2-deoxyglucose). Fluorescence intensity was measured at excitation wavelengths of 405 and 485 nm and emission wavelength of 508 nm. A calibration curve was constructed using buffers titrated to pH 4–8. Cells were incubated for 1 h at 30 °C in the presence of 75 μM monensin and 10 μM nigericin. A standard curve of fluorescence was generated and used to calculate the cytosolic pH from the observed fluorescence ratios.

Vacuolar pH was measured using the acetoxymethyl ester of 2′,7′-bis-(2-carboxyethyl)-5-,6-carboxyfluorescein (BCECF-AM) purchased from Life Technologies, Inc. Wild-type yeast cells were grown overnight to log phase in I− or I+ medium buffered to pH 5 with 50 mM sodium phosphate and 50 mM sodium succinate, with or without 0.6 mM VPA as indicated. Measurements of vacuolar pH were performed as described (53) except that after labeling with BCECF-AM and washing to remove excess label, cells were incubated with or without 2 μM concanamycin A for 15 min at room temperature in the absence of glucose.

FM4-64 Staining—To visualize vacuolar membranes *in vivo*, cells were stained with the lipophilic dye FM4-64 (Molecular Probes) as described (54) with slight modifications. Cells were grown overnight at 30 °C with constant shaking. One ml of culture was pelleted and resuspended in 300 μl of fresh medium containing 10 μM FM4-64 and 50 mM PIPES (pH 6.5). Cells were incubated for 30 min, harvested, washed twice, and chased in fresh medium for about 2 h. For microscopy, cells were pelleted and resuspended in a small volume of fresh medium. To immobilize cells, coverslips were coated with a thin layer of 1% agarose dissolved in SM. Cells were examined using a fluorescence microscope.

Vacuole Isolation and Biochemical Characterization—For experiments with the LN284 *ino1*Δ strain, cells were grown overnight in I+ medium to the mid-log phase. They were then washed and resuspended in I− buffered to pH 5 with 50 mM MES. For the I+ samples, cells were resuspended to a density of 0.3 A_{600}/ml (to allow for growth during the incubation), and 100 μM inositol was added. The I− samples were resuspended to 1.0 A_{600}/ml and showed little growth during the incubation. Both samples were incubated for 4 h at 30 °C with shaking. After incubation, cells from both types of experiments were converted to spheroplasts. Vacuolar vesicles were isolated through two Ficoll density gradient centrifugation steps as described (55).

Wild-type cells (BY4741) were grown overnight to log phase in I+ or I− medium buffered to pH 5 with 50 mM potassium phosphate and 50 mM potassium succinate, with or without 0.6 mM VPA added. Cells were converted to spheroplasts, and vacuolar vesicles were isolated as described above.

ATPase activity in isolated vacuolar vesicles was assessed by a coupled enzyme assay (56), and V-ATPase activity was determined by measuring ATPase activity in the presence and absence of the V-ATPase-specific inhibitor concanamycin A (Enzo Life Sciences). Total vacuolar protein was measured by the Lowry assay (57). Proton pumping was measured by the 9-amino-6-chloro-2-methoxyacridine fluorescence quenching assay (58). Pumping was initiated by addition of ATP and Mg^{2+} to final concentrations of 0.5 and 1 mM, respectively, and was inhibited by the addition of 100 nM concanamycin A. For immunoblotting, equal amounts of vacuolar vesicle protein were solubilized and separated on SDS-PAGE. The level of V-ATPase assembly was assessed on immunoblots probed with monoclonal antibodies 10D7 against V_0 subunit Vph1p and 8B1, 13D11, and 7A2 against V_1 subunits A, B, and C, respectively (59), followed by alkaline phosphatase-conjugated goat anti-mouse secondary antibody.

Fluorescence Microscopy—Imaging of yeast cells was performed using an Olympus BX41 epifluorescence microscope. Images were acquired using an Olympus Q-Color3, a digital charge-coupled device camera operated by QCapture2 software. The plasmids pRS415-FYVE-GFP used to localize PI3P and pRS416-Atg18-GFP used to localize $PI3,5P_2$ were the kind gifts from Dr. Scott Emr (Cornell University).

Electron Microscopy—Cells were grown in SM to the mid-log phase and processed as described previously (60). Briefly, cells were harvested, fixed in 3% glutaraldehyde, 0.1 M sodium cacodylate (pH 7.4), 5 mM $CaCl_2$, 5 mM $MgCl_2$, and 2.5% sucrose, stained with osmium thiocarbohydrazide, and subjected to EM analysis at the Integrated Imaging Center at Johns Hopkins University.

Statistical Analysis—Statistical comparisons of vacuolar pH and V-ATPase and proton pumping activities were performed using GraphPad QuickCalcs. Results from at least three independent experiments were subjected to a two-tailed unpaired *t* test. *p* values of less than 0.05 were designated as significant and less than 0.01 as highly significant. A one-way analysis of variance test was used to determine the effect of VPA on cytosolic pH.

Results

Mutants in Vacuolar Sorting and the V-ATPase Are Sensitive to VPA—VPA causes a decrease in inositol by inhibiting the enzyme that catalyzes the first and rate-limiting step of inositol biosynthesis (17, 18), yet the cellular consequences of inositol depletion caused by VPA have not been characterized. To identify mechanisms or pathways that may be perturbed by VPA, we screened the yeast deletion mutant collection to identify mutants exhibiting increased sensitivity to VPA. Cells were grown in the presence or absence of 2, 3, and 6 mM VPA, with or without 75 μM inositol. Growth was scored relative to that of wild-type cells. Of the 4,815 mutants screened, we found 84 mutants that were hypersensitive to VPA. They were classified into seven categories based on the reported functions of these genes according to the *Saccharomyces* Genome Database (Table 2). Group 1 consisted of 22 secretory pathway mutants, five of which were V-ATPase deletion (*vma*$^-$) mutants. These data suggest that mutants with defects in trafficking and vacuolar functions are particularly vulnerable to the effects of VPA.

VPA Perturbs the Vacuolar Structure as a Consequence of Inositol Depletion—The vacuolar structure is dependent on the delicate balance of solutes between the vacuolar and the cyto-

TABLE 2
Genes disrupted in mutants identified in the VPA-sensitivity screen (*vma* mutants are underlined)

	Group	Genes
1	Secretory pathway	*VMA3/CUP5, VPS67/VPS51, SAC2/VPS52, VPS53, LUV1/VPS54, SEC22, PEP12, STP22/VPS23, VPS25, BRO1/ VPS31, VPS66, VMA5, VMA21, VMA16/PPA1, VPH1, PMR1, MNN11, COG6, SAC1, BRE5, RVS167, RVS161,*
2.	Transcription complexes	*CCR4, TAF14, MOT2, POP2, SNF4*
3.	Ubiquitin-dependent proteolytic pathway	*MEP2, RPN4, DEF1, UBP3, BRE5,*
4.	Mitochondrial function	*AFG3, MGM101, MRPL27, MMT2, AIM13/MCS19*
5.	Transporters	*TRK1, CTR1, GUP1, HXT12, AQR1, TFP3, ATP15, RTC2, SPF1/COD1*
6.	Functionally unrelated (other)	*IRA1, NPL3, RMD7, SER2, PAC10, KAR3, NCL1, NPL6, BUB1, SPC72, MOG1, FYV6, SDL1, TRP1, NIS1, MKT1, CTK1, TRX3, RPL21A, ERF2, CAT2, GSH1, SLI15, NHP10, KEM1, SCS2, POC4, SLM4, EOS1, NCS2, KRE28, DCG1*
7.	Uncharacterized ORFs	*YIL090W, YCR061W, YJR018W, YIL166C, YNL120C, YML010W-A*

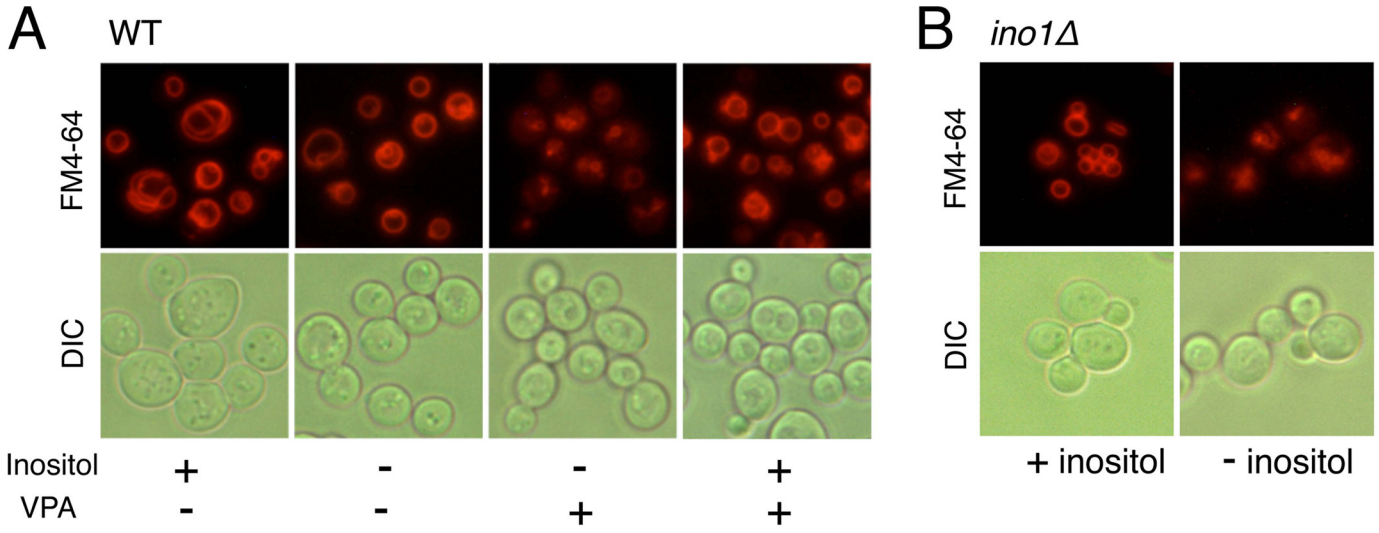

FIGURE 1. **Vacuolar defects in VPA-treated cells are rescued by supplementation with inositol.** *A*, VPA perturbs the vacuolar structure in wild-type cells. To determine the effects of VPA on vacuolar structure, wild-type cells were grown to the mid-log phase in SM with or without 1 mM VPA and 75 μM inositol. *B*, inositol starvation perturbs the vacuolar structure in *ino1*Δ cells. The effects of inositol starvation were determined in *ino1*Δ cells precultured in SM I+, washed twice to remove inositol, and resuspended in SM I−. Vacuoles were visualized by staining with FM4-64 as described under "Experimental Procedures." The results are representative of at least three independent experiments. *DIC*, differential interference contrast.

solic compartments. This balance is largely determined by the vacuolar membrane, which has a distinctive lipid composition (61) and a variety of protein pumps that transport ions and protons across the membrane (62). The proton gradient is maintained by the V-ATPase, which acidifies the vacuole. To determine whether VPA perturbs the vacuolar structure, wild-type cells were grown overnight in SM with or without inositol, in the presence or absence of VPA. In inositol-deficient medium (I−), VPA-treated cells exhibited decreased incorporation of FM4-64 (Fig. 1*A*), which enters the cells by endocytosis and labels the vacuolar membrane. In contrast, cells grown in the absence of VPA exhibited clear, well defined vacuoles. Inositol supplementation rescued the vacuolar defect of VPA-treated cells, suggesting that inositol depletion caused by VPA is responsible for perturbing the vacuolar membrane. To determine whether vacuolar perturbation is inositol-dependent, *ino1*Δ cells, which cannot synthesize inositol, were grown overnight in the presence of inositol (I+) and then switched to (I−) medium to induce inositol starvation. FM4-64 staining showed a pattern of vacuolar perturbation (Fig. 1*B*) similar to that observed in the VPA-treated cells (Fig. 1*A*). Taken together, these findings suggest that VPA perturbs vacuolar structure as a consequence of inositol depletion.

Perturbation of vacuolar structure was not sufficient to cause the *vma*$^-$ phenotype characteristic of V-ATPase mutants, *i.e.* sensitivity to high pH and high concentrations of calcium (39). As seen in Fig. 2*A*, VPA did not inhibit growth of wild-type cells under these conditions. Oluwatosin and Kane (63) reported that yeast cells must lose 70–75% of V-ATPase function to develop a *vma*$^-$ growth phenotype. Therefore, if perturbation of the vacuole by VPA resulted from inhibition of the V-ATPase, the loss of function was expected to be less than 70–75%.

Because only a subset of the *vma* mutants were identified in the screen for VPA sensitivity (Table 2), we further explored the sensitivity of other *vma* mutants to VPA, particularly those disrupting subunits of the membrane-bound V_0 sector. All of the *vma*Δ mutants tested showed sensitivity to VPA, which was rescued by inositol (Fig. 2*B*). *VPH1* and *STV1* encode two isoforms of the largest membrane subunit of the V-ATPase; single deletion mutants of these subunits exhibited modest VPA sensitivity that was rescued by inositol. These findings suggest that VPA triggers an inositol-dependent mechanism that increases sensitivity of the mutants to the drug. At least three possible mechanisms may explain this outcome. First, VPA may alter the cytosolic pH, which could exacerbate the defective pH

homeostasis of *vma*$^-$ mutants. To test this, we used a pHluorin-based assay (52) to measure the effect of VPA on cytosolic pH. Within the range of concentrations of VPA used therapeutically (0.6–2.0 mM), VPA did not alter the cytosolic pH (Fig. 3).

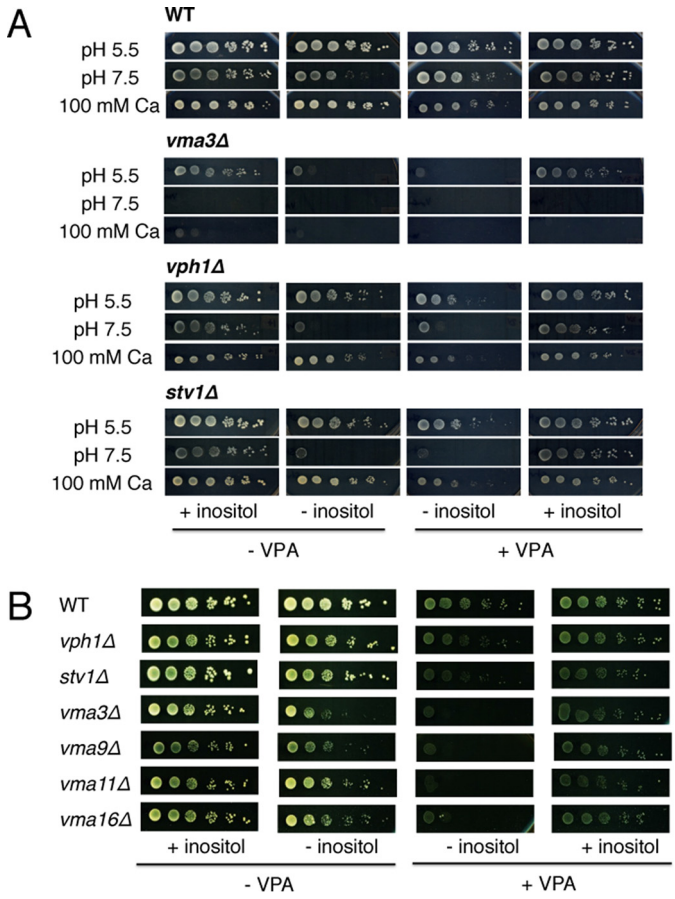

FIGURE 2. **VPA does not cause a *vma*$^-$ phenotype.** *A*, wild-type (*WT*) BY4741 and isogenic *vma3*Δ, *vph1*Δ, and *stv1*Δ mutant cells were precultured in SM I+, washed twice to remove inositol, and spotted in a 10-fold dilution series on SM in the presence or absence of 75 μM inositol and 2 mM VPA. Media were buffered to either pH 5.5 or 7.5. $CaCl_2$ (100 mM) was added to unbuffered medium. Cells were grown for 3–4 days at 30 °C. *B*, inositol rescues VPA sensitivity of V-ATPase V_0 deletion mutants. Wild-type (*WT*) BY4741 and isogenic *vma*Δ mutant cells were precultured in SM I+, washed twice to remove inositol, and spotted in a 10-fold dilution series on SM in the presence or absence of 75 μM inositol and 2 mM VPA. Cells were grown for 3–4 days at 30 °C. The experiments were done twice in duplicate.

A second possibility is that VPA triggers a mechanism that increases intracellular calcium levels, which inhibit growth of *vma*$^-$ mutants. This is not likely, as VPA does not appear to inhibit growth of wild-type cells in the presence of high Ca^{2+} (Fig. 2*A*). A third possibility is that VPA disrupts the synthesis of phosphoinositides that are essential for vacuolar function. This possibility was investigated further.

VPA Alters the Dynamics of Vacuolar PI3,5P$_2$—We addressed the possibility that VPA-induced inositol depletion affects PI3,5P_2, the key phosphoinositide of the vacuolar membrane. We have previously shown that VPA causes inositol depletion within the first few hours after addition to growing cells (64). To monitor the effect of VPA on the dynamics of PI3,5P_2, we visualized this phosphoinositide in the vacuolar membrane over a period of 4 h, using a GFP-tagged PI3,5P_2-binding probe containing an Atg18 domain (65) that specifically recognizes PI3,5P_2 (Fig. 4). Within the first 2 h, striking differences were observed between the treated and untreated cells (Fig. 4). VPA-treated cells showed punctate fluorescent structures on the vacuolar membrane, indicative of localized accumulation of PI3,5P_2 in those structures. These punctae persisted for a short time (less than an hour) and then gradually diminished as the vacuole grew in size. In the untreated cells, smaller punctae formed. Interestingly, however, the punctae rapidly developed into fluorescent and membranous bubble-like structures (*arrows* in Fig. 4), which protruded into the lumen of the original large vacuole. The protrusions formed septae that resulted in the fragmentation of the original large vacuole into multiple smaller ones. The intense fluorescence indicates that these membranes are enriched with PI3,5P_2, which suggests that vacuolar fission is preceded by a phase of increased PI3,5P_2 synthesis. This phenomenon was not observed in the VPA-treated cells, in which fluorescent membranes did not emerge out of punctae (as shown in the 2nd h). The vacuoles continued to increase in size for a few hours, after which the single enlarged vacuole started to diminish in size, rather than divide into multiple small vacuoles. Starvation for inositol in *ino1*Δ cells resulted in a similar phenotype, which was rescued by inositol (Fig. 4). These observations suggest that VPA perturbs the generation of PI3,5P_2-enriched membranes, possibly by decreasing the synthesis of PI3,5P_2 during the first

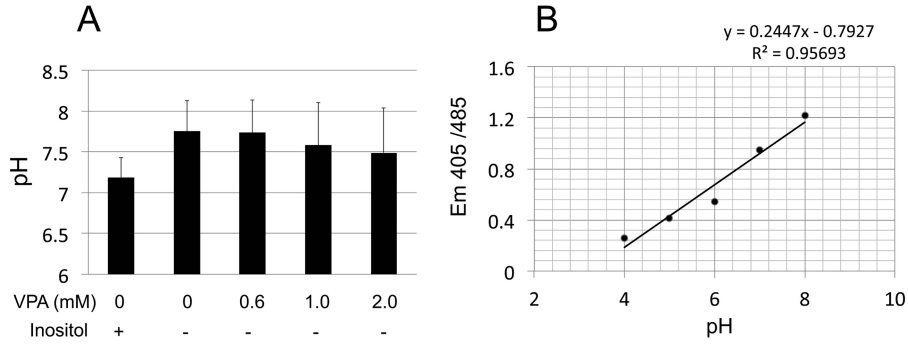

FIGURE 3. **Cytosolic pH is not altered by VPA treatment.** *A*, cytosolic pH was measured in wild-type cells expressing a pH-sensitive yeast pHluorin. Cells were grown to the mid-log phase in SM (*Ura*−) with or without 75 μM inositol and the indicated concentrations of VPA. Cells were harvested, washed, and resuspended in neutral buffer. Fluorescence intensity was measured at excitation wavelengths 405 and 485 nm and emission wavelength of 508 nm. *B*, calibration curve constructed using buffers titrated to pH 4–8 was used to convert the fluorescence values to cytosolic pH. Values represent the mean of three independent experiments ± S.E. (*error bars*). Analysis of variance was calculated to determine the effect of VPA and inositol on cytosolic pH. The analysis showed no significant difference $F(4,10) = 0.28$, $p = 0.87$.

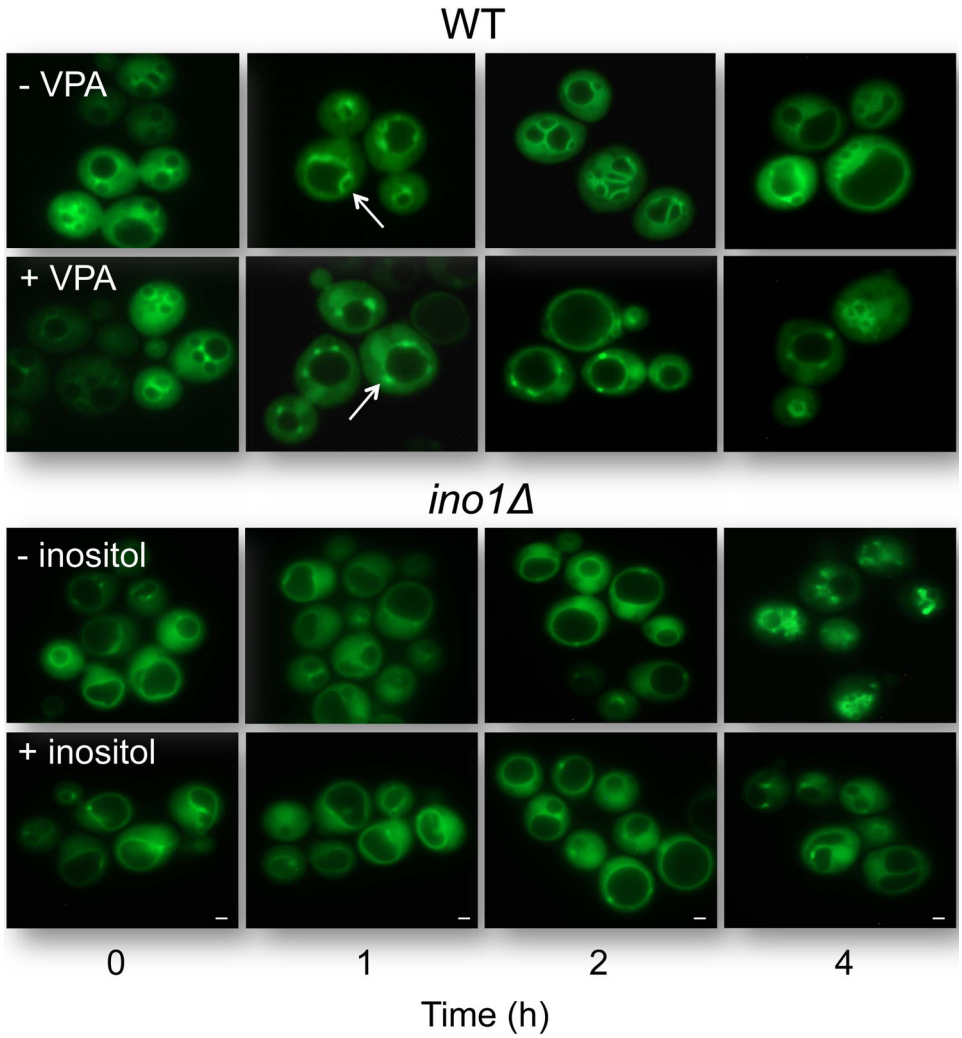

FIGURE 4. **VPA alters the dynamics of vacuolar PI3,5P$_2$.** Wild-type cells constitutively expressing a GFP-tagged PI3,5P$_2$-binding probe (Atg18-GFP) were grown in SM at 30 °C to the mid-log phase. VPA was added to a final concentration of 2 mM. *Ino1*Δ cells expressing the GFP-tagged PI3,5P$_2$-binding probe were initially grown in I+ medium and then transferred to inositol-deficient medium to initiate starvation. Cells were harvested at the indicated times following addition of the drug to WT or initiation of starvation in *ino1*Δ and visualized by fluorescence microscopy. *Arrows* point to punctae. *Scale bar*, 1 μm. The results are representative of at least three independent experiments.

2 h. As a consequence, the vacuoles do not undergo fission but remain enlarged, a phenotype similar to that of the *fab1*Δ mutant, which cannot synthesize PI3,5P$_2$ (66).

Electron microscopy (EM) analysis of cellular changes associated with VPA showed that the drug enhances formation of single enlarged vacuoles within the 1st h of exposure (Fig. 5, *A* and *B*). In this analysis, about 80% of VPA-treated cells showed single enlarged vacuoles compared with 20% in the untreated cells (Fig. 5, *A* and *B*). These results are consistent with the finding shown in Fig. 4, suggesting that VPA causes a phenotype consistent with compromised synthesis of PI3,5P$_2$.

VPA Limits the Increase in Fluorescence Associated with the PI3,5P$_2$ Probe in Response to Osmotic Stress—PI3,5P$_2$ is the least abundant of the phosphoinositides in eukaryotic cells, comprising less than 0.1% of all phosphoinositides (38). Decreased levels of PI3,5P$_2$ are associated with an increase in vacuolar size (66), whereas an increase in levels of PI3,5P$_2$ is associated with vacuolar fragmentation (67). Osmotic stress leads to a several-fold increase in levels of PI3,5P$_2$ (67, 68) and in the number of vacuoles per cell. To determine whether the vacuolar enlargement observed in VPA-treated cells is due to interrupted generation of PI3,5P$_2$, we exposed wild-type cells harboring the GFP-tagged PI3,5P$_2$-binding probe to osmotic stress and monitored the cells for accumulation of fluorescence. Although the untreated cells showed an increase in fluorescence within minutes of exposure to 0.9 M NaCl, significantly less fluorescence was observed in VPA-treated cells (Fig. 6*A*). The finding that osmotic stress, which normally causes an increase in PI3,5P$_2$ levels, does not cause a similar increase in VPA-treated cells suggests that VPA compromises the generation of PI3,5P$_2$.

Consistent with perturbation of PI3,5P$_2$ generation, osmotic stress did not induce vacuolar fragmentation in VPA-treated cells (Fig. 6*B*). Wild-type cells were exposed to 0.9 M NaCl in the presence or absence of VPA, and the number of vacuoles per cell was determined (Fig. 6*C*). For this purpose, about 100 cells were counted in each condition, and the percentage of cells with 1, 2–3, 4–5, or >5 vacuoles was calculated. In the absence of VPA, osmotic stress caused a shift toward a higher number of

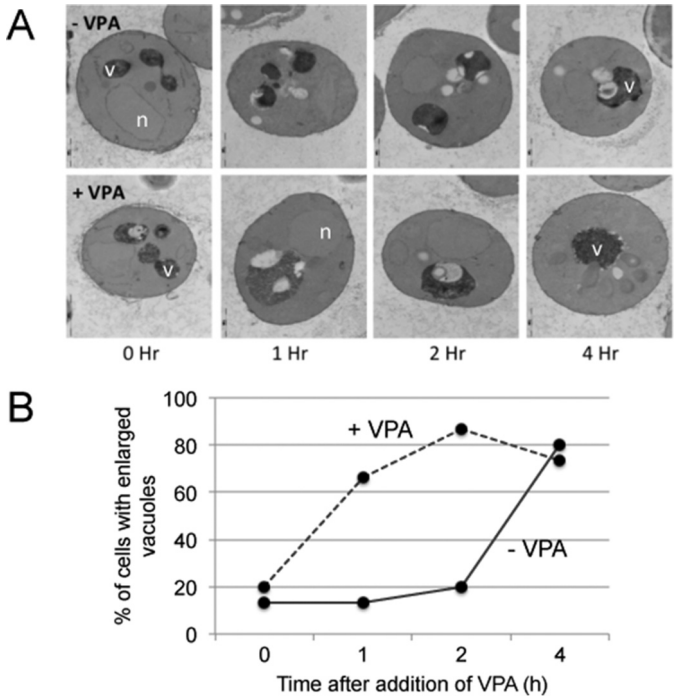

FIGURE 5. **VPA enhances formation of enlarged vacuoles.** *A*, electron micrographs of wild-type cells grown in SM to the mid-log phase and treated with VPA for the indicated times. *Upper panel*, untreated cells (−*VPA*); *bottom panel*, cells treated with 1 mM VPA (+*VPA*). *B*, percentage of cells with single enlarged vacuoles in VPA-treated cells was compared with that of untreated cells. A total of 120 cells were analyzed. *v*, vacuole; *n*, nucleus.

vacuoles per cell (Fig. 6*C*). In contrast, about 85% of VPA-treated cells had single vacuoles (Fig. 6*C*). This suggested that perturbation of $PI3,5P_2$ generation persists even under osmotic stress. Interestingly, when VPA-treated cells were kept under osmotic stress for about 2 h, total lysis of cells was observed. This suggests that VPA may cause cell wall defects or perturbation of the cell wall integrity pathway, rendering cells sensitive to the increased turgor pressure caused by the osmotic stress response. Alternatively, VPA may inhibit the osmotic stress response pathway. These findings suggest that VPA causes a constitutive decrease in $PI3,5P_2$, which cannot be rescued by increased osmotic stress.

To determine whether VPA-mediated perturbation of $PI3,5P_2$ is a consequence of decreased levels of PI3P (the precursor of $PI3,5P_2$), we visualized the changes in PI3P levels in response to VPA in *fab1*Δ cells transformed with a PI3P-specific GFP-tagged PI3P-binding probe (69). The *fab1*Δ mutant was used because PI3P localizes to the vacuole in the absence of *FAB1* (Fig. 6*D*). No obvious changes in PI3P levels were detected in the VPA-treated cells (Fig. 6*D*). This suggests that the decrease in $PI3,5P_2$ observed in the WT cells may be due to altered regulation of Fab1p or its regulators Vac7p and Vac14p, and not due to increased turnover of $PI3,5P_2$ into PI3P.

Inositol Deprivation and VPA Treatment Compromise V-ATPase Activity—V-ATPases catalyze ATP-driven proton transport resulting in organelle acidification and are central to multiple vacuolar functions. The sensitivity of the *vma* mutants to VPA (Fig. 2*B*) could reflect the effects of VPA on inositol biosynthesis but could also be less specific, as *vma* mutants are sensitive to multiple permeant weak acids (70). In support of inositol depletion affecting the V-ATPase, reduced PI3P and $PI3,5P_2$ levels compromise vacuolar acidification (67), and V-ATPase activity is regulated in response to $PI3,5P_2$ (51). Given the evidence above indicating that inositol deprivation affects a number of properties of the vacuole and exerts an effect on $PI3,5P_2$ generation, we next asked whether V-ATPase activity was compromised in cells acutely deprived of inositol. *ino1*Δ mutant cells lack the ability to synthesize inositol and thus are completely dependent on exogenous inositol. We deprived *ino1*Δ mutants of inositol for 4 h and then isolated vacuolar vesicles. As shown in Fig. 7*A*, inositol deprivation significantly reduced both ATP hydrolysis (by 59%) and proton pumping (by 77%) (Fig. 7*B*). V-ATPase activity is often regulated at the level of assembly, so we determined whether the loss of V-ATPase activity in the *ino1*Δ mutant was accompanied by disassembly of the peripheral V_1 from the membrane V_0 subunits. As shown in Fig. 7*C*, levels of vacuolar V_0 subunit Vph1 and V_1 subunits A–C from the vacuolar membrane were comparable in the presence and absence of inositol, suggesting that the V-ATPase remains assembled under inositol deprivation conditions (Fig. 7*C*).

Although wild-type yeast cells retain the ability to synthesize inositol and thus can grow in the absence of exogenous inositol, total cellular levels of inositol are reduced even when wild-type cells are grown in medium lacking inositol (71). To determine whether this reduced level of cellular inositol would have an effect on V-ATPase activity, we grew wild-type cells overnight in I− or I+ medium and then isolated vacuolar vesicles. As shown in Fig. 8, *A* and *B*, ATPase activity and proton pumping were modestly decreased in vacuolar membranes from wild-type cells grown under inositol deprivation conditions.

We hypothesized that if inositol deprivation affects V-ATPase activity, then VPA treatment, which compromises inositol biosynthesis, might also compromise V-ATPase function, particularly in the absence of exogenous inositol. To test this, wild-type cells were grown overnight in I+ or I− medium, with or without 0.6 mM VPA. VPA treatment had no significant effect on ATPase activity, as shown in Fig. 8*A*. However, VPA treatment in the absence of added inositol completely eliminated proton pumping in three independent preparations of vacuolar vesicles (Fig. 8*B*). Inositol supplementation reversed the effect of VPA on proton pumping, suggesting that VPA exerts its effects on the V-ATPase via inositol deprivation.

We next asked whether VPA treatment affects vacuolar pH using the fluorescent ratiometric pH indicator BCECF (53). Vacuolar pH in cells grown in I+ or I− medium was similar, and preincubation with the V-ATPase inhibitor concanamycin resulted in a significantly higher vacuolar pH, suggesting that V-ATPase activity is a major contributor to vacuolar acidification under these conditions (Fig. 9). Interestingly, VPA significantly reduced vacuolar pH, even in the presence of inositol. Because cytosolic pH is maintained in the presence of VPA (Fig. 3), this may suggest that the vacuole is sequestering the weak acid VPA, resulting in a drop in vacuolar pH. Vacuolar pH remained highly sensitive to V-ATPase inhibition in I+ medium containing VPA, however. In contrast, vacuolar pH was no longer sensitive to

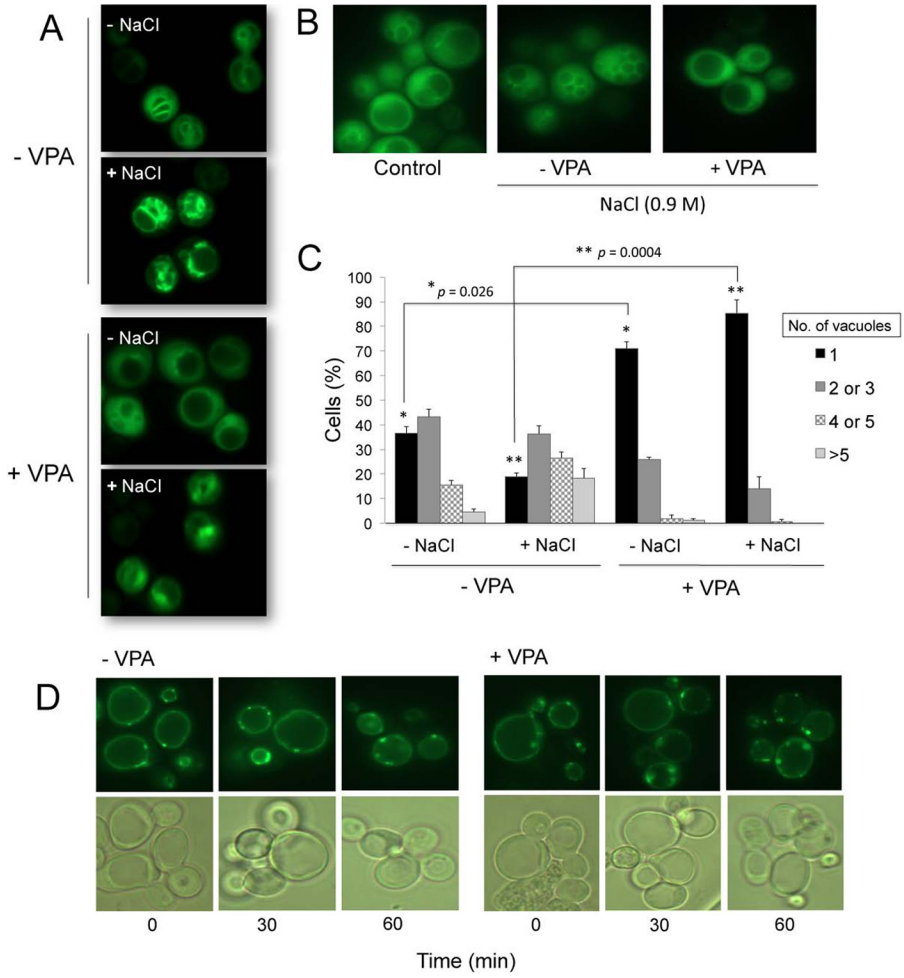

FIGURE 6. **PI3,5P$_2$ is perturbed in VPA-treated cells.** *A,* intensity of fluorescence associated with the PI3,5P$_2$-binding probe is higher in untreated cells (−*VPA*) following exposure to osmotic shock (+*NaCl*). Wild-type cells constitutively expressing the GFP-tagged PI3,5P$_2$-binding probe (Atg18-GFP) were grown in SM at 30 °C to the mid-log phase and treated with 2 mM VPA for 1 h. Cells were harvested and exposed to hyperosmotic stress for 5 min in SM to which NaCl was added to a final concentration of 0.9 M. Cells were observed by fluorescence microscopy. *B*, vacuolar fragmentation in response to hyperosmotic stress. *C*, vacuolar morphology of VPA-treated and -untreated cells was analyzed by fluorescence microscopy and quantified. The number of cells containing 1, 2–3, 4–5, or >5 vacuoles was determined. For each condition, about 100 cells were analyzed. The results are the mean of three independent experiments ± S.E. (*error bars*). Statistical analysis using a two-tailed unpaired *t* test indicated a significant effect of VPA on the number of cells with single vacuoles. *, $p = 0.026$ for (−*NaCl*), and **, $p = 0.0004$ for (+*NaCl*). *D*, Wild-type cells constitutively expressing a GFP-tagged PI3P-binding probe (FYVE-GFP) were grown in SM at 30 °C to the mid-log phase. VPA was added to a final concentration of 2 mM. Cells were harvested at the indicated times following addition of the drug and visualized by fluorescence microscopy.

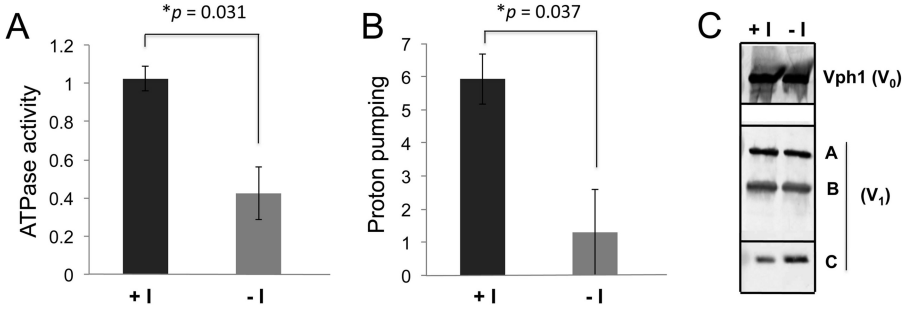

FIGURE 7. **Inositol depletion inhibits V-ATPase activity and reduces H$^+$ pumping in *ino1*Δ cells.** *ino1*Δ cells were grown in SM I+ buffered to pH 5 overnight and then washed twice and resuspended in either SM I+ or SM I−, both buffered to pH 5, and incubated for 4 h at 30 °C. Vacuolar vesicles were isolated as described under "Experimental Procedures." *A,* mean concanamycin A-sensitive ATPase activity (in μmol of ATP hydrolyzed per min/mg of protein) for three independent vacuole preparations is shown. *Error bars* represent S.E. *B*, proton pumping rate was assayed using the ACMA fluorescence-quenching assay as described under "Experimental Procedures." Results represent the mean ± S.E. for three independent vacuole preparations. *p* values for significant differences based on unpaired two-tailed *t* test are indicated. *C,* immunoblots of vacuoles were probed for V$_0$ subunit Vph1 and V$_1$ subunits *A–C* as described under "Experimental Procedures." 7 μg of vacuolar protein were loaded for detection of Vph1 and subunit C, and 5 μg were loaded for detection of the A and B subunits.

concanamycin A in cells grown in I− medium containing VPA. This is consistent with the absence of V-ATPase-driven proton pumping in isolated vacuolar vesicles from these cells (Fig. 8*B*), and this suggests that inositol-deprived cells treated with VPA can achieve an acidic vacuolar pH, but without a significant contribution from the V-ATPase.

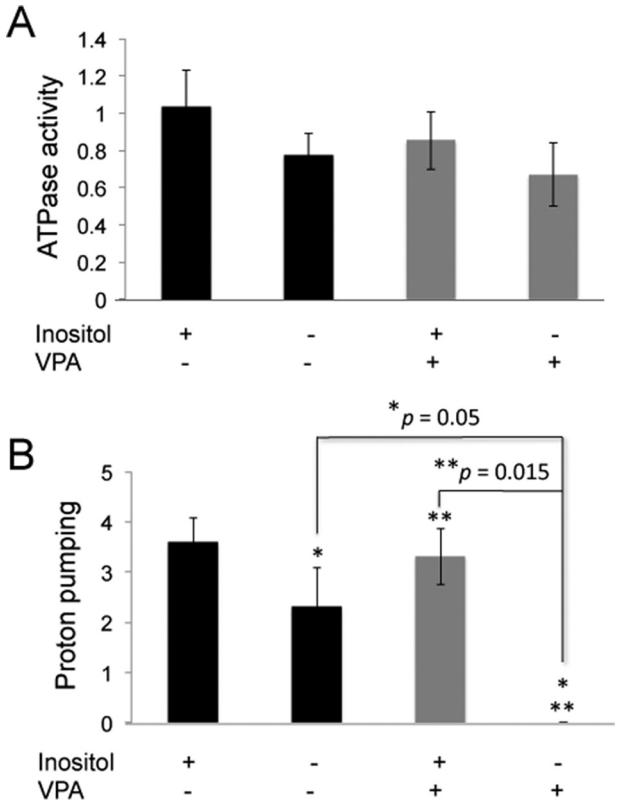

FIGURE 8. **VPA results in an inositol-reversible loss of H^+ pumping in vacuolar vesicles from wild-type cells.** WT cells were grown overnight, with or without 100 μM inositol and 0.6 mM VPA in SM buffered to pH 5 with 50 mM potassium phosphate and 50 mM potassium succinate. Vacuolar vesicles were isolated as described under "Experimental Procedures." *A*, concanamycin A-sensitive ATPase activity was measured in vacuolar vesicles isolated from cells grown overnight in the presence or absence of inositol and VPA as indicated. The mean activity (in μmol of ATP/min/mg protein) of four independent preparations from cells grown in I+ or I− medium without VPA and three independent preparations from VPA-treated cells is shown, and *error bars* indicate S.E. There were no significant differences between the V-ATPase activities between the four different conditions. *B*, initial rate of proton pumping was measured in the same preparations of vacuolar vesicles and the mean ± S.E. × 10^4 is shown. Three independent preparations of vacuolar vesicles from cells grown in the presence of VPA and the absence of inositol showed no proton pumping. *p* values for significant differences based on unpaired two-tailed *t* test are indicated.

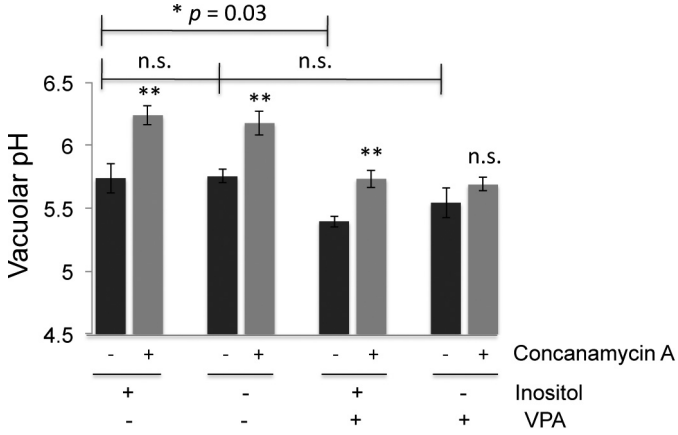

FIGURE 9. **Vacuolar pH was measured using BCECF.** Cells were grown to log phase overnight in the indicated medium buffered to pH 5 with 50 mM potassium phosphate and 50 mM potassium succinate. Cells were briefly deprived of glucose, and then vacuolar pH was averaged over a period of 100 s, starting 8 min after glucose re-addition. *Black bars* represent the mean of four independent experiments, with *error bars* corresponding to the standard error of the mean. *Gray bars* correspond to the means of paired samples incubated with the V-ATPase inhibitor concanamycin A for 15 min before glucose re-addition. Statistical comparison (unpaired *t* test) of I+ samples grown overnight with and without VPA indicated a significant difference with $p = 0.03$. There was no significant (*n.s.*) difference between I+ and I− samples ($p = 0.94$) or I− samples grown with or without valproate present ($p = 0.29$). The average vacuolar pH in the presence and absence of concanamycin A was also compared for each sample. All of the samples except the I−, VPA+ sample showed highly significant differences between concanamycin-treated (*gray bars*) and -untreated (*black bars*) (**, $p = 0.005$–0.009). There was not a significant difference ($p = 0.12$) with concanamycin A treatment of the cells grown in I− medium with VPA.

Discussion

This study shows for the first time that both inositol depletion and VPA perturb the V-ATPase. We report the following novel findings. 1) Inositol depletion by VPA or starvation of *ino1*Δ cells leads to perturbation of vacuolar structure. 2) VPA perturbs $PI3,5P_2$ generation and leads to an increase in vacuolar size. These perturbations are not rescued by osmotic stress, which normally up-regulates $PI3,5P_2$ synthesis. 3) Inositol starvation significantly reduces V-ATPase activity and proton pumping. 4) VPA significantly reduces V-ATPase proton pumping under inositol-limiting conditions. Taken together, these findings identify novel consequences of inositol depletion and provide evidence for a previously unidentified link between inositol and the V-ATPase.

The finding that inositol starvation perturbs the vacuole (Fig. 1) and reduces V-ATPase activity and proton pumping (Fig. 7) indicates that cellular inositol levels impact V-ATPase function. The V-ATPase responds to multiple environmental cues. The V_0/V_1 complex disassembles in response to glucose deprivation (72). This work is the first to show that inositol is capable of modulating activity of the V-ATPase. One possible mechanism to explain this is based on the availability of Glc-6-P, a substrate that can drive either the inositol biosynthesis pathway or the glycolytic pathway. In the absence of exogenous inositol, *de novo* biosynthesis of inositol is activated, using Glc-6-P as the substrate for *myo*-inositol-3-phosphate synthase to generate inositol 3-P, which is subsequently dephosphorylated to produce inositol. However, when inositol is supplied in the medium, *de novo* biosynthesis of inositol is repressed, and thus more Glc-6-P is available for the glycolytic pathway; hence, more ATP is generated. Therefore, it is possible that increased V-ATPase activity observed in the presence of inositol (Figs. 7 and 8) is ultimately due to the availability of Glc-6-P required for glycolysis, ATP generation, and full V-ATPase assembly. However, it should be noted that V-ATPase assembly did not appear to change during acute inositol deprivation in the *ino1*Δ cells (Fig. 7*C*). This suggests that inositol deprivation exerts an effect on the V-ATPase that does not require disassembly of V_1 from V_0. Recent evidence suggests that even in conditions that reduce V-ATPase activity, such as glucose deprivation, many of the V_1 subunits may remain loosely associated with the membrane (73). It is therefore possible that inositol deprivation generates changes in V_1-V_0 interactions that do not result in full release of V_1 subunits. A more plausible explanation is based on the decrease in phosphoinositide levels under inositol-limiting conditions (7, 9). The observation that inositol rescued the perturbation of the vacuolar membrane in inositol-starved and VPA-treated cells (Fig. 1, *A* and *B*) suggests that decreased

V-ATPase activity is due to a membrane defect, which supports the role of phosphoinositides. It was previously suggested that V-ATPase activity may be modulated by the phosphoinositide $PI3,5P_2$ (34, 35), and Li *et al.* (51) reported that the V-ATPase is stabilized and activated by $PI3,5P_2$. In support of the role of $PI3,5P_2$ in regulation of V-ATPase activity, the *fab1*Δ mutant, which cannot synthesize $PI3,5P_2$, has decreased V-ATPase activity (51) and enlarged vacuoles (66). These phenotypes are very similar to those caused by VPA. We therefore hypothesize that inositol depletion caused by VPA alters the levels of $PI3,5P_2$, in the vacuolar membrane, and thereby causes a decrease in V-ATPase function.

The use of the GFP-tagged $PI3,5P_2$-binding probe enabled us to monitor changes in the localization and relative abundance of $PI3,5P_2$ over time and under different conditions. The observation that VPA-treated cells exhibit vacuolar enlargement suggests that VPA causes a decrease in $PI3,5P_2$ levels. This could be a consequence of altered synthesis or turnover of this phosphoinositide. The inability of VPA-treated cells to increase $PI3,5P_2$ in response to osmotic shock (Fig. 6) further supports perturbation of $PI3,5P_2$ metabolism by VPA. It is well documented that hyperosmotic shock triggers a 20-fold increase in levels of $PI3,5P_2$ along with an increase in vacuole number (67, 68). However, the mechanism underlying this response is undetermined (74). Osmotically shocked VPA-treated cells did not show the same level of increase in $PI3,5P_2$ as the untreated cells (Fig. 6*A*). Consistent with this, osmotic shock of VPA-treated cells did not trigger an increase in the number of vacuoles, in contrast to untreated cells in which ~80% of osmotically shocked cells showed multiple vacuoles (Fig. 6, *B* and *C*). Taken together, these findings suggest that VPA impairs $PI3,5P_2$ generation and that this impairment persists even under osmotic stress.

One possible consequence of impaired $PI3,5P_2$ homeostasis is perturbation of the binding between $PI3,5P_2$ and the V-ATPase, possibly triggering a conformational change in the membrane-embedded V_0 sector and accounting for reduced H^+ pumping (Figs. 7*B* and 8*B*). Chan *et al.* (75) have shown that the tether region joining the cytosolic and membrane domains of Vph1 is critical for pharmacological uncoupling of the V-ATPase. Therefore, it is possible that altered levels of $PI3,5P_2$ may partially disturb this region, causing a functional uncoupling of the V-ATPase without the dissociation of the V_1 complex seen in *fab1*Δ and *vac14*Δ cells (51). Alternatively, $PI3,5P_2$ may bind or recruit factors required for activation of the V-ATPase.

The changes in membrane dynamics that preceded vacuolar fission were intriguing (Fig. 4). The emergence of $PI3,5P_2$-enriched membranes from the localized dense formations on the vacuolar membrane suggests that an increase in $PI3,5P_2$ generation is a prerequisite for vacuolar fission, as several small vacuoles could be seen following protrusion of the $PI3,5P_2$-packed membranes into the vacuolar space (Fig. 4). Zieger and Mayer (76) reported similar structures, which they referred to as "membranous structures devoid of protein." The findings that protrusions did not form in the VPA-treated cells (+*VPA*, Fig. 4) and that the vacuoles did not divide, but instead fused together and enlarged (Figs. 4 and 5, *A* and *B*), are consistent with perturbation of $PI3,5P_2$ homeostasis by VPA, and they suggest that a consequence of this perturbation is failure of the vacuoles to divide into multiple smaller vacuoles. It is tempting to speculate that the changes in $PI3,5P_2$ dynamics could identify a novel role for $PI3,5P_2$ whereby a transient increase in this phosphoinositide initiates vacuole fission, which otherwise does not occur in mutants that lack $PI3,5P_2$.

The finding that V-ATPase pumping is greatly reduced in vacuolar vesicles from VPA-treated cells grown under inositol-limiting conditions suggested that the vacuolar pH may be increased as a consequence. Surprisingly, BCECF measurements showed that vacuolar pH was significantly reduced in VPA-treated cells irrespective of V-ATPase activity, suggesting that VPA, a weak acid, may be sequestered in the vacuole. This may render these cells sensitive to stresses that challenge organelle acidification, in which V-ATPase activation helps to maintain organelle pH. For example, Ho *et al.* (77) recently showed that vacuolar pH could be maintained at near-normal levels in a *fab1*Δ mutant, which has compromised V-ATPase activity, but that vacuolar pH was not stable during salt shock in the mutant. In summary, our findings suggest that inositol depletion and VPA perturb $PI3,5P_2$ generation resulting in decreased V-ATPase function and perturbation of the vacuole.

Implications for the Therapeutic Effect of VPA—The V-ATPase plays an essential role in the acidification and proper function of intracellular compartments, including lysosomes, secretory vesicles, and synaptic vesicles. The proton gradient generated by the V-ATPase is utilized in the uploading and storage of neurotransmitters (78). Specific inhibition of V-ATPase activity has been shown to block uptake of L-glutamate and γ-aminobutyric acid into vesicles (79, 80). Several neurotransmitter receptor blockers have been shown to dissipate the pH gradient established by the V-ATPase, thereby altering the uptake of dopamine, γ-aminobutyric acid, and glutamate (81). A number of studies indicate that neurotransmission is altered in response to VPA (82–85). However, the mechanism whereby VPA elicits this effect is not known. Here, we show a mechanistic link between inositol depletion caused by VPA and perturbation of the V-ATPase. The functional conservation between vesicular trafficking in yeast and synaptic vesicle trafficking in mammalian neurons suggests that our findings may be pertinent to altered neurotransmission and may thus shed light on a novel mechanism of action of VPA.

In conclusion, our study shows that both inositol depletion and VPA treatment lead to impairment of V-ATPase function and altered dynamics of vacuolar $PI3,5P_2$. This is the first demonstration of a link between inositol depletion and the V-ATPase. We speculate that altered levels of $PI3,5P_2$ in the vacuolar membrane as a consequence of inositol depletion may disrupt the conformational structure of the V_0 sector of the V-ATPase, impairing the efficiency of V-ATPase function. Although there appear to be additional effects of VPA on organelle acidification, weak acid effects are less likely to be physiologically relevant in mammalian cells, where the extracellular pH tends to be much higher than that of fungi. Therefore, we propose that therapeutic effects of inositol depletion caused by VPA may be mediated in part by effects on V-ATPases.

Author Contributions—R. M. D. designed and carried out all the experiments in Figs. 1–4 and 6, the data analysis in Fig. 5, and wrote the manuscript. Y. S. carried out the initial screen for VPA-sensitive mutants. Y. C. carried out preliminary experiments with FM4-64 that suggested that the V-ATPase might be perturbed. J. M. M. did the EM imaging. M. T. performed the V-ATPase and BCECF assays. P. M. K. coordinated and analyzed the V-ATPase experiments in Figs. 7–9, and contributed to the writing. M. L. G. conceived and coordinated the study and contributed to the writing and editing of the manuscript.

Acknowledgments—We thank Dr. Rajini Rao and Dr. Scott Emr for kind gifts of plasmids. We also thank Dr. Stephen Jesch for thoughtful comments and suggestions.

References

1. Jesch, S. A., Liu, P., Zhao, X., Wells, M. T., and Henry, S. A. (2006) Multiple endoplasmic reticulum-to-nucleus signaling pathways coordinate phospholipid metabolism with gene expression by distinct mechanisms. *J. Biol. Chem.* **281,** 24070–24083
2. Jesch, S. A., Zhao, X., Wells, M. T., and Henry, S. A. (2005) Genome-wide analysis reveals inositol, not choline, as the major effector of Ino2p-Ino4p and unfolded protein response target gene expression in yeast. *J. Biol. Chem.* **280,** 9106–9118
3. Santiago, T. C., and Mamoun, C. B. (2003) Genome expression analysis in yeast reveals novel transcriptional regulation by inositol and choline and new regulatory functions for Opi1p, Ino2p, and Ino4p. *J. Biol. Chem.* **278,** 38723–38730
4. Henry, S. A., Gaspar, M. L., and Jesch, S. A. (2014) The response to inositol: regulation of glycerolipid metabolism and stress response signaling in yeast. *Chem. Phys. Lipids* **180,** 23–43
5. Deranieh, R. M., and Greenberg, M. L. (2009) Cellular consequences of inositol depletion. *Biochem. Soc. Trans.* **37,** 1099–1103
6. Gaspar, M. L., Aregullin, M. A., Jesch, S. A., and Henry, S. A. (2006) Inositol induces a profound alteration in the pattern and rate of synthesis and turnover of membrane lipids in *Saccharomyces cerevisiae*. *J. Biol. Chem.* **281,** 22773–22785
7. Henry, S. A., Atkinson, K. D., Kolat, A. I., and Culbertson, M. R. (1977) Growth and metabolism of inositol-starved *Saccharomyces cerevisiae*. *J. Bacteriol.* **130,** 472–484
8. Becker, G. W., and Lester, R. L. (1977) Changes in phospholipids of *Saccharomyces cerevisiae* associated with inositol-less death. *J. Biol. Chem.* **252,** 8684–8691
9. Hanson, B. A., and Lester, R. L. (1980) Effects of inositol starvation on phospholipid and glycan syntheses in *Saccharomyces cerevisiae*. *J. Bacteriol.* **142,** 79–89
10. Cox, J. S., Chapman, R. E., and Walter, P. (1997) The unfolded protein response coordinates the production of endoplasmic reticulum protein and endoplasmic reticulum membrane. *Mol. Biol. Cell* **8,** 1805–1814
11. Chang, H. J., Jones, E. W., and Henry, S. A. (2002) Role of the unfolded protein response pathway in regulation of INO1 and in the sec14 bypass mechanism in *Saccharomyces cerevisiae*. *Genetics* **162,** 29–43
12. Jesch, S. A., Gaspar, M. L., Stefan, C. J., Aregullin, M. A., and Henry, S. A. (2010) Interruption of inositol sphingolipid synthesis triggers Stt4p-dependent protein kinase C signaling. *J. Biol. Chem.* **285,** 41947–41960
13. Berridge, M. J. (1989) Inositol 1,4,5-trisphosphate-induced calcium mobilization is localized in *Xenopus* oocytes. *Proc. R. Soc. Lond. B Biol. Sci.* **238,** 235–243
14. Perucca, E. (2002) Pharmacological and therapeutic properties of valproate: a summary after 35 years of clinical experience. *CNS Drugs* **16,** 695–714
15. Bowden, C. L., and McElroy, S. L. (1995) History of the development of valproate for treatment of bipolar disorder. *J. Clin. Psychiatry* **56,** 3–5
16. Calabresi, P., Galletti, F., Rossi, C., Sarchielli, P., and Cupini, L. M. (2007) Antiepileptic drugs in migraine: from clinical aspects to cellular mechanisms. *Trends Pharmacol. Sci.* **28,** 188–195
17. Vaden, D. L., Ding, D., Peterson, B., and Greenberg, M. L. (2001) Lithium and valproate decrease inositol mass and increase expression of the yeast INO1 and INO2 genes for inositol biosynthesis. *J. Biol. Chem.* **276,** 15466–15471
18. Deranieh, R. M., He, Q., Caruso, J. A., and Greenberg, M. L. (2013) Phosphorylation regulates myo-inositol-3-phosphate synthase: a novel regulatory mechanism of inositol biosynthesis. *J. Biol. Chem.* **288,** 26822–26833
19. Belmaker, R. H. (2004) Bipolar disorder. *N. Engl. J. Med.* **351,** 476–486
20. McLaurin, J., Franklin, T., Chakrabartty, A., and Fraser, P. E. (1998) Phosphatidylinositol and inositol involvement in Alzheimer amyloid-β fibril growth and arrest. *J. Mol. Biol.* **278,** 183–194
21. Shimohama, S., Tanino, H., Sumida, Y., Tsuda, J., and Fujimoto, S. (1998) Alteration of myo-inositol monophosphatase in Alzheimer's disease brains. *Neurosci. Lett.* **245,** 159–162
22. Lowe, M. (2005) Structure and function of the Lowe syndrome protein OCRL1. *Traffic* **6,** 711–719
23. Taylor, G. S., Maehama, T., and Dixon, J. E. (2000) Myotubularin, a protein-tyrosine phosphatase mutated in myotubular myopathy, dephosphorylates the lipid second messenger, phosphatidylinositol 3-phosphate. *Proc. Natl. Acad. Sci. U.S.A.* **97,** 8910–8915
24. Clément, S., Krause, U., Desmedt, F., Tanti, J. F., Behrends, J., Pesesse, X., Sasaki, T., Penninger, J., Doherty, M., Malaisse, W., Dumont, J. E., Le Marchand-Brustel, Y., Erneux, C., Hue, L., and Schurmans, S. (2001) The lipid phosphatase SHIP2 controls insulin sensitivity. *Nature* **409,** 92–97
25. Marion, E., Kaisaki, P. J., Pouillon, V., Gueydan, C., Levy, J. C., Bodson, A., Krzentowski, G., Daubresse, J. C., Mockel, J., Behrends, J., Servais, G., Szpirer, C., Kruys, V., Gauguier, D., and Schurmans, S. (2002) The gene INPPL1, encoding the lipid phosphatase SHIP2, is a candidate for type 2 diabetes in rat and man. *Diabetes* **51,** 2012–2017
26. Chow, C. Y., Landers, J. E., Bergren, S. K., Sapp, P. C., Grant, A. E., Jones, J. M., Everett, L., Lenk, G. M., McKenna-Yasek, D. M., Weisman, L. S., Figlewicz, D., Brown, R. H., and Meisler, M. H. (2009) Deleterious variants of FIG 4, a phosphoinositide phosphatase, in patients with ALS. *Am. J. Hum. Genet.* **84,** 85–88
27. Kotoulas, A., Kokotas, H., Kopsidas, K., Droutsas, K., Grigoriadou, M., Bajrami, H., Schorderet, D. F., and Petersen, M. B. (2011) A novel PIKFYVE mutation in fleck corneal dystrophy. *Mol. Vis.* **17,** 2776–2781
28. Strahl, T., and Thorner, J. (2007) Synthesis and function of membrane phosphoinositides in budding yeast, *Saccharomyces cerevisiae*. *Biochim. Biophys. Acta* **1771,** 353–404
29. Cooke, F. T., Dove, S. K., McEwen, R. K., Painter, G., Holmes, A. B., Hall, M. N., Michell, R. H., and Parker, P. J. (1998) The stress-activated phosphatidylinositol 3-phosphate 5-kinase Fab1p is essential for vacuole function in *S. cerevisiae*. *Curr. Biol.* **8,** 1219–1222
30. Gary, J. D., Sato, T. K., Stefan, C. J., Bonangelino, C. J., Weisman, L. S., and Emr, S. D. (2002) Regulation of Fab1 phosphatidylinositol 3-phosphate 5-kinase pathway by Vac7 protein and Fig 4, a polyphosphoinositide phosphatase family member. *Mol. Biol. Cell* **13,** 1238–1251
31. Sbrissa, D., Ikonomov, O. C., and Shisheva, A. (1999) PIKfyve, a mammalian ortholog of yeast Fab1p lipid kinase, synthesizes 5-phosphoinositides. Effect of insulin. *J. Biol. Chem.* **274,** 21589–21597
32. Duex, J. E., Tang, F., and Weisman, L. S. (2006) The Vac14p-Fig 4p complex acts independently of Vac7p and couples PI3,5P2 synthesis and turnover. *J. Cell Biol.* **172,** 693–704
33. Botelho, R. J., Efe, J. A., Teis, D., and Emr, S. D. (2008) Assembly of a Fab1 phosphoinositide kinase signaling complex requires the Fig 4 phosphoinositide phosphatase. *Mol. Biol. Cell* **19,** 4273–4286
34. Weisman, L. S. (2003) Yeast vacuole inheritance and dynamics. *Annu. Rev. Genet.* **37,** 435–460
35. Baars, T. L., Petri, S., Peters, C., and Mayer, A. (2007) Role of the V-ATPase in regulation of the vacuolar fission-fusion equilibrium. *Mol. Biol. Cell* **18,** 3873–3882
36. Efe, J. A., Botelho, R. J., and Emr, S. D. (2005) The Fab1 phosphatidylinositol kinase pathway in the regulation of vacuole morphology. *Curr. Opin. Cell Biol.* **17,** 402–408
37. Odorizzi, G., Babst, M., and Emr, S. D. (2000) Phosphoinositide signaling and the regulation of membrane trafficking in yeast. *Trends Biochem. Sci.*

25, 229–235
38. Michell, R. H., Heath, V. L., Lemmon, M. A., and Dove, S. K. (2006) Phosphatidylinositol 3,5-bisphosphate: metabolism and cellular functions. *Trends Biochem. Sci.* **31,** 52–63
39. Kane, P. M. (2006) The where, when, and how of organelle acidification by the yeast vacuolar H^+-ATPase. *Microbiol. Mol. Biol. Rev.* **70,** 177–191
40. Kane, P. M. (2007) The long physiological reach of the yeast vacuolar H^+-ATPase. *J. Bioenerg. Biomembr.* **39,** 415–421
41. Breton, S., and Brown, D. (2007) New insights into the regulation of V-ATPase-dependent proton secretion. *Am. J. Physiol. Renal Physiol.* **292,** F1–F10
42. Blair, H. C., Teitelbaum, S. L., Ghiselli, R., and Gluck, S. (1989) Osteoclastic bone resorption by a polarized vacuolar proton pump. *Science* **245,** 855–857
43. Kartner, N., Yao, Y., Li, K., Crasto, G. J., Datti, A., and Manolson, M. F. (2010) Inhibition of osteoclast bone resorption by disrupting vacuolar H^+-ATPase a3-B2 subunit interaction. *J. Biol. Chem.* **285,** 37476–37490
44. Brown, D., Paunescu, T. G., Breton, S., and Marshansky, V. (2009) Regulation of the V-ATPase in kidney epithelial cells: dual role in acid-base homeostasis and vesicle trafficking. *J. Exp. Biol.* **212,** 1762–1772
45. El Far, O., and Seagar, M. (2011) A role for V-ATPase subunits in synaptic vesicle fusion? *J. Neurochem.* **117,** 603–612
46. El Far, O., and Seagar, M. (2011) SNARE, V-ATPase and neurotransmission. *Medecine Sciences* **27,** 28–31
47. Zhang, Z., Nguyen, K. T., Barrett, E. F., and David, G. (2010) Vesicular ATPase inserted into the plasma membrane of motor terminals by exocytosis alkalinizes cytosolic pH and facilitates endocytosis. *Neuron* **68,** 1097–1108
48. Hiesinger, P. R., Fayyazuddin, A., Mehta, S. Q., Rosenmund, T., Schulze, K. L., Zhai, R. G., Verstreken, P., Cao, Y., Zhou, Y., Kunz, J., and Bellen, H. J. (2005) The v-ATPase V0 subunit a1 is required for a late step in synaptic vesicle exocytosis in *Drosophila*. *Cell* **121,** 607–620
49. Di Giovanni, J., Boudkkazi, S., Mochida, S., Bialowas, A., Samari, N., Lévêque, C., Youssouf, F., Brechet, A., Iborra, C., Maulet, Y., Moutot, N., Debanne, D., Seagar, M., and El Far, O. (2010) V-ATPase membrane sector associates with synaptobrevin to modulate neurotransmitter release. *Neuron* **67,** 268–279
50. Poëa-Guyon, S., Ammar, M. R., Erard, M., Amar, M., Moreau, A. W., Fossier, P., Gleize, V., Vitale, N., and Morel, N. (2013) The V-ATPase membrane domain is a sensor of granular pH that controls the exocytotic machinery. *J. Cell Biol.* **203,** 283–298
51. Li, S. C., Diakov, T. T., Xu, T., Tarsio, M., Zhu, W., Couoh-Cardel, S., Weisman, L. S., and Kane, P. M. (2014) The signaling lipid PI(3,5)P2 stabilizes V_1-V_0 sector interactions and activates the V-ATPase. *Mol. Biol. Cell* **25,** 1251–1262
52. Orij, R., Postmus, J., Ter Beek, A., Brul, S., and Smits, G. J. (2009) *In vivo* measurement of cytosolic and mitochondrial pH using a pH-sensitive GFP derivative in *Saccharomyces cerevisiae* reveals a relation between intracellular pH and growth. *Microbiology* **155,** 268–278
53. Diakov, T. T., Tarsio, M., and Kane, P. M. (2013) Measurement of vacuolar and cytosolic pH *in vivo* in yeast cell suspensions. *J. Vis. Exp.* 10.3791/50261
54. Vida, T. A., and Emr, S. D. (1995) A new vital stain for visualizing vacuolar membrane dynamics and endocytosis in yeast. *J. Cell Biol.* **128,** 779–792
55. Roberts, C. J., Raymond, C. K., Yamashiro, C. T., and Stevens, T. H. (1991) Methods for studying the yeast vacuole. *Methods Enzymol.* **194,** 644–661
56. Lötscher, H. R., deJong, C., and Capaldi, R. A. (1984) Interconversion of high and low adenosine triphosphatase activity forms of *Escherichia coli* F1 by the detergent lauryldimethylamine oxide. *Biochemistry* **23,** 4140–4143
57. Lowry, O. H., Rosebrough, N. J., Farr, A. L., and Randall, R. J. (1951) Protein measurement with the Folin phenol reagent. *J. Biol. Chem.* **193,** 265–275
58. Liu, M., Tarsio, M., Charsky, C. M., and Kane, P. M. (2005) Structural and functional separation of the N- and C-terminal domains of the yeast V-ATPase subunit H. *J. Biol. Chem.* **280,** 36978–36985
59. Kane, P. M., Kuehn, M. C., Howald-Stevenson, I., and Stevens, T. H. (1992) Assembly and targeting of peripheral and integral membrane subunits of the yeast vacuolar H^+-ATPase. *J. Biol. Chem.* **267,** 447–454
60. Rieder, S. E., Banta, L. M., Köhrer, K., McCaffery, J. M., and Emr, S. D. (1996) Multilamellar endosome-like compartment accumulates in the yeast vps28 vacuolar protein sorting mutant. *Mol. Biol. Cell* **7,** 985–999
61. Li, S. C., and Kane, P. M. (2009) The yeast lysosome-like vacuole: endpoint and crossroads. *Biochim. Biophys. Acta* **1793,** 650–663
62. Cagnac, O., Aranda-Sicilia, M. N., Leterrier, M., Rodriguez-Rosales, M. P., and Venema, K. (2010) Vacuolar cation/H^+ antiporters of *Saccharomyces cerevisiae*. *J. Biol. Chem.* **285,** 33914–33922
63. Oluwatosin, Y. E., and Kane, P. M. (1998) Mutations in the yeast KEX2 gene cause a Vma(−)-like phenotype: a possible role for the Kex2 endoprotease in vacuolar acidification. *Mol. Cell. Biol.* **18,** 1534–1543
64. Ju, S., and Greenberg, M. L. (2003) Valproate disrupts regulation of inositol responsive genes and alters regulation of phospholipid biosynthesis. *Mol. Microbiol.* **49,** 1595–1603
65. Dove, S. K., Piper, R. C., McEwen, R. K., Yu, J. W., King, M. C., Hughes, D. C., Thuring, J., Holmes, A. B., Cooke, F. T., Michell, R. H., Parker, P. J., and Lemmon, M. A. (2004) Svp1p defines a family of phosphatidylinositol 3,5-bisphosphate effectors. *EMBO J.* **23,** 1922–1933
66. Yamamoto, A., DeWald, D. B., Boronenkov, I. V., Anderson, R. A., Emr, S. D., and Koshland, D. (1995) Novel PI(4)P 5-kinase homologue, Fab1p, essential for normal vacuole function and morphology in yeast. *Mol. Biol. Cell* **6,** 525–539
67. Bonangelino, C. J., Nau, J. J., Duex, J. E., Brinkman, M., Wurmser, A. E., Gary, J. D., Emr, S. D., and Weisman, L. S. (2002) Osmotic stress-induced increase of phosphatidylinositol 3,5-bisphosphate requires Vac14p, an activator of the lipid kinase Fab1p. *J. Cell Biol.* **156,** 1015–1028
68. Dove, S. K., Cooke, F. T., Douglas, M. R., Sayers, L. G., Parker, P. J., and Michell, R. H. (1997) Osmotic stress activates phosphatidylinositol 3,5-bisphosphate synthesis. *Nature* **390,** 187–192
69. Burd, C. G., and Emr, S. D. (1998) Phosphatidylinositol(3)-phosphate signaling mediated by specific binding to RING FYVE domains. *Mol. Cell* **2,** 157–162
70. Mira, N. P., Teixeira, M. C., and Sá-Correia, I. (2010) Adaptive response and tolerance to weak acids in *Saccharomyces cerevisiae*: a genome-wide view. *Omics* **14,** 525–540
71. Jiranek, V., Graves, J. A., and Henry, S. A. (1998) Pleiotropic effects of the opi1 regulatory mutation of yeast: its effects on growth and on phospholipid and inositol metabolism. *Microbiology* **144,** 2739–2748
72. Kane, P. M. (1995) Disassembly and reassembly of the yeast vacuolar H(+)-ATPase *in vivo*. *J. Biol. Chem.* **270,** 17025–17032
73. Tabke, K., Albertmelcher, A., Vitavska, O., Huss, M., Schmitz, H. P., and Wieczorek, H. (2014) Reversible disassembly of the yeast V-ATPase revisited under *in vivo* conditions. *Biochem. J.* **462,** 185–197
74. Michell, R. H. (2013) Inositol lipids: from an archaeal origin to phosphatidylinositol 3,5-bisphosphate faults in human disease. *FEBS J.* **280,** 6281–6294
75. Chan, C. Y., Prudom, C., Raines, S. M., Charkhzarrin, S., Melman, S. D., De Haro, L. P., Allen, C., Lee, S. A., Sklar, L. A., and Parra, K. J. (2012) Inhibitors of V-ATPase proton transport reveal uncoupling functions of tether linking cytosolic and membrane domains of V0 subunit a (Vph1p). *J. Biol. Chem.* **287,** 10236–10250
76. Zieger, M., and Mayer, A. (2012) Yeast vacuoles fragment in an asymmetrical two-phase process with distinct protein requirements. *Mol. Biol. Cell* **23,** 3438–3449
77. Ho, C. Y., Choy, C. H., Wattson, C. A., Johnson, D. E., and Botelho, R. J. (2015) The Fab1/PIKfyve phosphoinositide phosphate kinase is not necessary to maintain the pH of lysosomes and of the yeast vacuole. *J. Biol. Chem.* **290,** 9919–9928
78. Schuldiner, S., Shirvan, A., and Linial, M. (1995) Vesicular neurotransmitter transporters: from bacteria to humans. *Physiol. Rev.* **75,** 369–392
79. Moriyama, Y., Maeda, M., and Futai, M. (1990) Energy coupling of L-glutamate transport and vacuolar H(+)-ATPase in brain synaptic vesicles. *J. Biochem.* **108,** 689–693
80. Hell, J. W., Maycox, P. R., Stadler, H., and Jahn, R. (1988) Uptake of GABA by rat brain synaptic vesicles isolated by a new procedure. *EMBO J.* **7,** 3023–3029
81. Moriyama, Y., Maeda, M., and Futai, M. (1992) The role of V-ATPase in

neuronal and endocrine systems. *J. Exp. Biol.* **172,** 171–178
82. Cunningham, M. O., Woodhall, G. L., and Jones, R. S. (2003) Valproate modifies spontaneous excitation and inhibition at cortical synapses *in vitro*. *Neuropharmacology* **45,** 907–917
83. Martín, E. D., and Pozo, M. A. (2004) Valproate reduced synaptic activity increase induced by 4-aminopyridine at the hippocampal CA3-CA1 synapse. *Epilepsia* **45,** 436–440
84. Martín, E. D., and Pozo, M. A. (2004) Valproate reduced excitatory postsynaptic currents in hippocampal CA1 pyramidal neurons. *Neuropharmacology* **46,** 555–561
85. Yoshida, S., Yamamura, S., Ohoyama, K., Nakagawa, M., Motomura, E., Kaneko, S., and Okada, M. (2010) Effects of valproate on neurotransmission associated with ryanodine receptors. *Neurosci. Res.* **68,** 322–328
86. Jiang, F., Rizavi, H. S., and Greenberg, M. L. (1997) Cardiolipin is not essential for the growth of *Saccharomyces cerevisiae* on fermentable or non-fermentable carbon sources. *Mol. Microbiol.* **26,** 481–491
87. Nunez, L. R., Jesch, S. A., Gaspar, M. L., Almaguer, C., Villa-Garcia, M., Ruiz-Noriega, M., Patton-Vogt, J., and Henry, S. A. (2008) Cell wall integrity MAPK pathway is essential for lipid homeostasis. *J. Biol. Chem.* **283,** 34204–34217